

Title page

Title

Pore mutations in the human kidney chloride channel ClC-Ka provide new insight into the mechanism of anion selectivity in the CLC protein family

Running title

Anion selectivity in ClC-Ka

Authors

Laura Lagostena¹, Giovanni Zifarelli^{2*}, Alessandra Picollo^{1*}

¹ Dulbecco Telethon Laboratory, Istituto di Biofisica, CNR, Genova, Italy.

² Department of Physiology, Anatomy and Genetics, University of Oxford, Oxford, UK.

* Corresponding authors:

Giovanni Zifarelli

Address: Parks Road, OX1 3PT Oxford, UK

Telephone: +44 01865272498

Email: giovanni.zifarelli@dpag.ox.ac.uk

Alessandra Picollo

Address: Via De Marini 6, I-16149 Genova, Italy

Telephone: +39 0106475649

Email: apicollo@dti.telethon.it

Key words: kidney, ClC-Ka, Bartter syndrome, chloride channel, anion selectivity, permeation.

Abstract word count: 237

Text word count: 2973

Significance Statement

The human chloride channels ClC-Ka and -Kb in complex with their accessory subunit Barttin are essential for NaCl reabsorption in the nephron and endolymph secretion in the inner ear. Mutations of ClC-Ks and Barttin cause type III and IV Bartter syndrome, characterized by renal salt wasting, hypokalemic metabolic alkalosis, and hypercalciuria with risk of kidney stones and hearing-loss. In this study, by electrophysiological techniques and mutational analysis we show that the mechanism of anion discrimination in the human ClC-Ka channel is unique in the CLC protein family and we identified new residues responsible for anion selectivity. This represents a fundamental progress in the understanding of the function of ClC-Ks channels and of CLC proteins in general.

Abstract

Background. The mechanism of anion selectivity in the human kidney chloride channels ClC-Ka and -Kb is thought to be very similar to the one of other channels and antiporters of the CLC protein family and to rely on the interaction of anions with a conserved Ser residue, Ser_{cen}, at the central of three binding sites in the permeation pathway, S_{cen}. In both CLC channels and antiporters mutations of Ser_{cen} alter the anion selectivity and in structures of CLC channels and antiporters, the side chain of Ser_{cen} projects into the pore and coordinate the anion bound at S_{cen}.

Methods. To investigate the role of several residues in anion selectivity of ClC-Ka we used amino acids substitutions and assessed the properties of the mutants by electrophysiological techniques.

Results. Mutations of Ser_{cen} to Gly, Pro and Thr do not have any effect on anion selectivity whereas the mutations Y425A, F519A and Y520A increase the NO₃⁻/Cl⁻ permeability ratio with a particularly strong effect of Y425A for which the wild-type preference for Cl⁻ over NO₃⁻ is reversed.

Conclusions. The mechanism of anion selectivity in ClC-Ka is largely independent of Ser_{cen} and it is therefore unique in the CLC protein family. We identified Y425 as a new residue contributing to anion discrimination in ClC-Ka and ClC-0. This work provides an important and timely insight into the relation between structure and function for the kidney channels ClC-Ka and -Kb and CLC proteins in general.

Introduction

The CLC protein family comprises chloride channels and anion/proton antiporters found in all phyla from bacteria to humans where they have a critical role in muscle excitability, ionic homeostasis of intracellular organelles and transepithelial transport as proved by their involvement in genetic diseases and the phenotype of knock-out mice ^{1, 2}. In particular, the closely related CLC-Ka and -Kb channels are expressed in the kidney ^{3, 4} and inner ear ⁵ where they are essential for transepithelial NaCl reabsorption ⁶ and the production of endolymph ⁷, respectively. They associate with the accessory protein barttin, which is essential for their expression in the plasma membrane ⁵ but also modulates the gating properties and sensitivity to Ca^{2+} and niflumic acid of both CLC-K isoforms ⁸⁻¹¹. Loss-of-function mutations of CLC-Kb result in severe salt loss (Bartter syndrome type III) ¹² while mutations in barttin cause a more severe form of Bartter syndrome (type IV) with the addition of congenital deafness ¹³. A similar phenotype is found in rare patients with mutations in both CLC-Ks ¹⁴. CLC-Ka as well as CLC-Kb polymorphisms have been associated with predisposition to hypertension ^{15, 16}. Knockout of CLC-K1 in mice leads to a defect in urinary concentration resembling the phenotype of human nephrogenic diabetes insipidus ¹⁷. In contrast, knock-out of CLC-K2 in mice results in a phenotype that is very similar to Bartter syndrome in humans ^{18, 19} confirming the notion that rodent CLC-K1/CLC-K2 corresponds to human CLC-Ka/CLC-Kb, respectively.

Structural studies and extensive functional analysis on both CLC channels and antiporters indicated that in spite of very different transport mechanisms channels and antiporters share a very similar structure. They are formed by dimers with each subunit comprising an independent permeation pathway with three anion binding sites, S_{ext} , S_{cen} and S_{int} (from the extracellular to the intracellular side, respectively) ²⁰⁻²⁴. S_{ext} and S_{cen} can be occupied either by an anion or by the side chain of a glutamate residue, located at the extracellular entry of the permeation pathway and called “gating” glutamate ²⁰⁻²². In CLC-1 this residue is captured in a different conformation with its side chain directed off to the side of the permeation pathway ²⁴. Mutations of the gating glutamate abolish both fast and slow gating transitions in CLC channels ^{1, 2} and in CLC antiporters additionally ablate H^+ transport turning them into uncoupled Cl^- conductances ^{21, 25-28}. Interestingly, this residue is conserved in most CLC proteins but is a Val in CLC-Ka and -Kb explaining their reduced gating relaxations. At S_{cen} anions are coordinated by the main chain nitrogen atoms of residues of the re-entrant loop $\alpha\text{M}-\alpha\text{N}$ (Ile 356 and Phe 357 in the bacterial EcCLC-1 and Y425 and F426 in CLC-Ka) and by the side chains of two conserved residues, Ser_{cen} and Tyr_{cen} forming a narrow constriction of the pore between S_{cen} and S_{int} ^{20-22, 24}. Mutations of Ser_{cen} deeply affect selectivity in both CLC

channels and transporters. Substitution of Ser_{cen} with Pro turned the Cl⁻/H⁺ antiporters CIC-5 and EcCIC-1 into NO₃⁻/H⁺ antiporters^{29, 30}. The plant NO₃⁻/H⁺ antiporter AtCIC-a has a Pro residue instead of Ser_{cen} and only poorly transports Cl⁻³¹ but substitution of the Pro_{cen} with a Ser turns the protein into a Cl⁻/H⁺ antiporter^{32, 33}. In CIC-0 the corresponding mutation (S123P) changed the wild-type preference for Cl⁻ over NO₃⁻^{30, 32}. Anion selectivity was also affected by the more conservative mutation S123T, although less dramatically³⁴. Halide selectivity was also drastically affected mutating Ser_{cen} (S168) to Cys in CIC-1³⁵. This large amount of work bolstered the conclusion that Ser_{cen} is the only determinant of the selectivity of CLC channels and transporters, even though the structural interpretation of these findings was based only on structures of CLC antiporters and the role of other residues forming S_{cen} was not interrogated. The recently obtained cryo-electron microscopy structures of the human CIC-1²⁴ and the bovine bCIC-K²³, orthologue of the human CIC-Ks channels, has offered the opportunity to directly test this interpretation on CLC channels for the first time. Indeed, while the structure of CIC-1 is in general similar to the one of the CLC antiporters in the region around S_{cen}, the structure of bCIC-K indicates major differences of the central binding site compared to the antiporters due to a different conformation of the loop αC-αD²³. As a result Ser_{cen} does not contribute to anion coordination at S_{cen} as it is further apart from Tyr_{cen} and its side chain points away from the pore (Fig. 1 A). Moreover, unique to bCIC-K, additional anion/quadrupole interactions at S_{cen} are provided by Y425 and F519²³ (Fig. 1 A). Interestingly, the sequence alignment of CIC-Ka and several other CLC channels and transporters in Fig. 1 B shows that Y425 and F519 are poorly conserved and CIC-Ka and -Kb are the only proteins with aromatic residues at that position. On the other end, the position of the anion bound at S_{cen} and the orientation of Tyr_{cen} as well as its role in anion coordination are substantially conserved in bCIC-K²³. These elements raise interesting questions regarding the mechanism of anion selectivity in CIC-Ks and other CLC proteins, particularly considering that CIC-Ks channels have an anion selectivity sequence similar to CIC-0 and all the other CLC channels. In this work, by two electrode voltage-clamp (TEVC), patch-clamp and mutational analysis we probed the role in anion selectivity of CIC-Ka of Ser_{cen} (S121) and of the other residues predicted by the bCIC-K structure to contribute to anion coordination at S_{cen}: Y425A, F519A and Tyr_{cen} (Y520 in CIC-Ka).

Material and Methods

Molecular biology and heterologous expression

DNA of human CIC-Ka and Torpedo CIC-0 were cloned in the PTLN vector for expression in oocytes³⁶, and in the pcDNA3 vector for expression in HEK293 cells. Mutations were introduced by recombinant PCR as described previously³⁷. For CLC-0, all mutations were introduced in the

background of the C212S mutation that eliminates the slow gate³⁸. cRNA of ClC-Ka and ClC-0 was transcribed from cDNA linearized with MluI with the mMessage mMachine SP6 kit (Ambion, Life Technologies, Italy), whereas cRNA of Y98A Barttin was transcribed from cDNA linearized with NotI with the mMessage mMachine T7 kit (Ambion). Wild-type and mutants of ClC-Ka were co-expressed with Barttin in a molar ratio of 1:5. For transfection in HEK293 cells 300-500 ng of ClC-Ka constructs was co-transfected with 150-300 ng of Barttin tagged with GFP at its C-terminus. HEK293 cells were cultured with DMEM, 1% glutamine, 1% penicillin/streptomycin, and 10% of FBS (all from Euroclone, Milano, Italy).

Electrophysiology

cRNA (about 50 ng) was injected in defolliculated *Xenopus* oocytes kept at 18°C in Barth's solution containing (in mM) 90 NaCl, 2 KCl, 1 CaCl₂ and 10 Hepes, pH 7.5. Two-three days after injection two-electrode voltage clamp (TEVC) measurements were performed with a Turbo TEC_03X amplifier (npi electronic, Tamm, Germany). Extracellular solution contained (in mM) 90 NaCl (substituted by equimolar amount of NaNO₃, NaBr and NaI for measurements of anion selectivity), 1 MgSO₄, 10 Ca-gluconate and 10 Hepes at pH 7.3. For ClC-Ka, the voltage protocol consisted of a 100 ms prepulse at + 60 mV followed by 200 ms steps to various test values (from -140 to + 80 mV with 20 mV increments). For ClC-0, the voltage protocol consisted of a 50 ms prepulse followed by 100 ms voltage steps from -160 mV to 80 mV with 20 mV. For TEVC experiments the holding potential was the membrane resting potential.

For patch-clamp experiments pipettes were pulled from borosilicates glass capillaries (Hilgenberg, Malsfeld, Germany) and had a resistance of 2-3 MΩ in recording solutions. The extracellular solution contained (in mM): 145 NaCl (or NaNO₃), 2 CaCl₂, 1 MgCl₂, and 10 Hepes at pH 7.3. The intracellular solution contained (in mM): 130 CsCl, 2 EGTA, 2 MgCl₂ and Hepes at pH 7.3. Pulses were elicited from a holding potential of 0 mV for 5 ms, followed by voltage steps from -120 mV to 80 mV with 20 mV increments for 100 ms and followed by a 40 mV pulse for 20 ms. Data were acquired at 50 kHz after filtering at 10 kHz with an eight-pole Bessel filter using an Axopatch 200 amplifier (Molecular Devices, San Jose, CA). All data were acquired at room temperature with the custom acquisition program GePulse and analyzed with the custom program Ana (both available at: <http://users.ge.ibf.cnr.it/pusch/>) and SigmaPlot (Systat Software, Hounslow, UK). Molecular models were produced with the program Pymol (Schrödinger Inc., OR). The ClC-Ka mutations of S121 to Ala, Glu, Gly, Pro and Thr did not sufficiently expressed in *Xenopus* oocytes (data not shown) but the mutations to Gly, Pro and Thr expressed in HEK cells. Wild-type ClC-Ka expression in HEK cells was much higher than in oocytes, consistent with previous work by other

groups pointing to an increased P_{open} of ClC-Ka and -Kb in cells (reviewed in Imbrici et al.)³⁹. The mechanism underlying this effect of the expression system on gating is still unclear³⁹. To assess anion selectivity, for each ionic condition the reversal potential of the currents, V_{rev} , was extrapolated fitting the steady state I-V curves with a polynomial function and used to calculate the relative permeability of anion to chloride (P_{anion}/P_{Cl^-}) using the following equation:

$$\frac{P_{anion}}{P_{Cl}} = \exp \left((V_{rev}(anion) - V_{rev}(Cl)) * F/RT \right)$$

where F is the Faraday constant, R is the gas constant and T is absolute temperature.

Statistical analysis

Results are presented as mean \pm SEM. Statistical analysis was performed using unpaired Student's *t* test with p values indicated in the figure legends. The number of independent experiments is indicated by "n".

Results

We first investigated the effect of Ser_{cen} substitutions in ClC-Ka. In patch-clamp experiments on HEK293 cells the mutations S121G, T and P display measurable time independent currents in Cl⁻ solution that remained much smaller compared to wild-type (Fig. 2). Cl⁻ substitution with NO₃⁻ reduces the currents of the wild-type and the mutants in a similar manner with a stronger effect at positive voltages (Fig. 2 and 3 A). Moreover, we found that $P_{NO_3^-}/P_{Cl^-}$ was not affected by any of the mutations of S121 (Fig. 3 B). We also tested the effect on anion selectivity of Ser_{cen} substitutions in ClC-0 and found that S123A and S123G profoundly affect $P_{NO_3^-}/P_{Cl^-}$ (Suppl. fig. 1).

We next investigated the role in ClC-Ka selectivity of Y425, F519 and Y520 with TEVC as all the constructs produced robust currents upon expression in oocytes. For the wild-type the effect of Cl⁻ substitution with NO₃⁻ at positive voltages is a decrease of the currents (Fig. 4) of comparable extent (but less pronounced) to the one that was observed in patch-clamp experiments (compare Fig. 3 A and 5 A) whereas at negative voltages currents in NO₃⁻ are slightly increased and show a profound change in kinetics not observed in HEK cells. In spite of these differences, the value of $P_{NO_3^-}/P_{Cl^-}$ for the wild-type is almost identical when measured in oocytes and HEK cells (0.26 and

0.32, respectively) (Fig. 3 B and 5 B) proving that it is fully justified to directly compare the measurements on anion selectivity performed in the two expression systems. Regarding the mutants, upon NO_3^- substitution the currents at positive voltages of F519A and Y520A decrease much more than for wild-type leading to an almost complete block for Y520A. Surprisingly, NO_3^- has the opposite effect on Y425A and currents are increased rather than decreased ($I_{\text{NO}_3^-}/I_{\text{Cl}^-}$ at +80 mV is 0.65 and 1.3 for wild-type and Y425, respectively) (Fig. 4 and 5 A). Compared to wild-type the $\text{NO}_3^-/\text{Cl}^-$ permeability ratio is progressively increased for F519A and Y520A and is more than doubled for Y425A. F519A and Y520A also significantly decreased $P_{\text{Br}^-}/P_{\text{Cl}^-}$ to 0.99 and 0.80, respectively (wild-type value is 1.1) leading to an inversion of Br^- vs Cl^- selectivity (Fig. 4 and Suppl. Table 1). Consistently, currents in Br^- are reduced compared to wild-type (Fig. 4 and Suppl. fig. 3). In addition the mutants show very little (Y425A and Y520A) or no (F519A) kinetic relaxations suggesting rather dramatic effects on gating (Fig. 4). For Y520A this was also accompanied by a marked increase in the level of functional expression.

Considering the interplay between gating and permeation in CLC proteins we performed an additional control experiment to rule out the possibility that our results on anion selectivity could be influenced by the altered gating introduced by the mutations or due to the expression system. To this end, we assessed the anion selectivity also for the N257A mutant (Suppl. fig. 2 A). This residue is located in the external loop between α -helices I and J, far removed for the permeation pathway (Fig. 1 A, shown in dark red) but it is known to substantially increase $\text{ClC-Ka } P_{\text{open}}^{40}$. The value of $P_{\text{NO}_3^-}/P_{\text{Cl}^-}$ is almost identical for wild-type and N257A (0.26 and 0.27, respectively) indicating that in spite of the pronounced difference in gating the permeability properties are not changed in this mutant. This supports the notion that our results on Y425A, F519A and Y520A, particularly the effect on $P_{\text{NO}_3^-}/P_{\text{Cl}^-}$, are not due to the altered gating of these mutants or to unspecific changes introduced by the expression system. Thus, we conclude that Y425 plays a central role in determining the anion selectivity of ClC-Ka with a less prominent role of F519A and Y520A.

Interestingly we found that the corresponding residue in ClC-0 (A417) also has an effect on selectivity. Compared to wild-type, the A417Y mutation has a similar behavior in Cl^- solution but a faster gating kinetics at negative voltages (Fig. 6). However, upon NO_3^- substitution A417Y has the opposite behavior compared to wild-type and currents are largely unaffected or increased. The relative $\text{NO}_3^-/\text{Cl}^-$ permeability is also significantly increased in A417Y compared to wild-type (0.58 and 0.69, respectively) potentially accounting for the different effect of NO_3^- on macroscopic currents.

Discussion

Several lines of evidence cemented the view that the mechanism of anion selectivity is almost identical across channels and transporters of the CLC protein family and rely on the conserved Ser_{cen}. In contrast to this view we found here that in CLC-Ka substitutions of Ser_{cen} (S121) to Gly, Pro and Thr do not affect the Cl⁻ over NO₃⁻ discrimination of the wild-type. This result is particularly straightforward in the case of S121P considering that in the channel CLC-0 and the antiporters EcCLC-1 and CLC-5 the same substitution of Ser_{cen} led to an inversion of the wild-type Cl⁻ vs NO₃⁻ selectivity. However, it is in agreement with the recent structure of bCLC-K showing that Ser_{cen} adopt a different conformation compared to CLC antiporters and does not contribute to anion coordination at S_{cen}²³. However, our results also lead to the conclusion that the structure and/or function of Ser_{cen} and the mechanism of anion selectivity differs between CLC-Ka and other CLC channels. This conclusion is directly supported by the finding that in CLC-1 the position of Ser_{cen} is almost identical as in CLC antiporters²⁴.

Moreover we found that Y425 and to a lesser extent F519 and Y520 are important in determining the anion selectivity. Y425 corresponds to I356 in EcCLC-1 and in the structure of this antiporter was recognized as a residue that also contributes to anion coordination but by main chain amide nitrogen atom in EcCLC-1²¹ whereas in bCLC-K Y425 projects its side chain into the permeation pathway engulfing the anion at the central binding site and providing dipole/quadrupole interactions through its aromatic ring²³. Intriguingly, CLC-K channels are the only human CLC proteins with aromatic residues at the positions corresponding to 425 and 519. Considering that to the best of our knowledge the role of the corresponding residue in anion selectivity of other CLC proteins has never been explored, we tested its function in CLC-0. Indeed, whereas for wild-type CLC-0 currents in NO₃⁻ are very small compared to Cl⁻, for the mutant A417Y the currents in NO₃⁻ are larger than in Cl⁻ and in addition the relative NO₃⁻/Cl⁻ permeability is significantly increased. This indicates an important functional role of this residue in selectivity in both CLC-Ka (as Y425) and CLC-0 (as A417). However this role is not identical as the opposite substitution (Y425A in CLC-Ka and A417Y in CLC-0) led to the same effect on anion selectivity, i.e. increase of NO₃⁻ vs. Cl⁻ permeability. This further supports the notion that the detailed mechanism underlying anion discrimination in CLC-Ka and CLC-0 is different. Interestingly, the corresponding residue in CLC-1 (G483) was identified as a critical determinant of the wider intracellular part of the pore compared to antiporters in spite of the conserved position of Ser_{cen} projecting into the pore.^{20-22, 24}.

The role of Tyr_{cen} in anion selectivity, although not prominent, appears unique to CLC-Ka, as studies in CLC-0 and CLC-1 suggested that Tyr_{cen} does not contribute to pore properties (selectivity and conductance). In fact in CLC-0 there was no effect of the mutations Y512A and Y512F on halide

selectivity and no effect on single-channel conductance at physiological anion concentrations^{37, 41}. Similar results were obtained in ClC-1 for the mutations Y578A and Y578W⁴².

Interestingly, Y520A also abolishes gating relaxations suggesting that besides affecting selectivity it also changes the gating properties of ClC-Ka. This is consistent with results obtained in ClC-0 and ClC-1 showing that Tyr_{cen} have an effect on fast gating^{37, 42, 43}. Interestingly, more recently, Bennetts et al. showed that mutations of this residue in ClC-0 and ClC-1 have a large effect on the slow gate and suggested that the interaction between gating glutamate and Tyr_{cen} might be the molecular determinant of slow gate in these channels⁴⁴. ClC-Ka lacks the gating glutamate (the corresponding residue is a Val) that in ClC-0 and ClC-1 is largely responsible for fast gating. However, gating relaxations in ClC-Ka are strongly reduced but not abolished. Interestingly, the effect we observed here for Y520A on current kinetics is similar to effect seen in ClC-0 and ClC-1 for Tyr_{cen} substitutions which abrogate the slow gate⁴⁴. On this basis, it is tempting to speculate that the residual gating observed in wild-type ClC-Ka is related to the slow gate of ClC-0 and ClC-1. However, further studies are required to draw firm conclusions on this point.

In summary our work shows that the mechanism of anion selectivity in ClC-Ka is independent of the conserved Ser_{cen} residue that determines the selectivity in all other CLC channels and transporters. We identified Y425 as a new residue with a role in selectivity in both ClC-Ka and ClC-0. Also in contrast to other CLC channels the mutation of Tyr_{cen} to Ala has an impact on anion selectivity. Our results are consistent with the structure of bClC-K, the first one of a CLC channel, but they indicate potentially important differences in the role of the conserved Ser and Tyr residues at S_{cen} between ClC-Ka and other CLC channels, a conclusion confirmed by the very recent structure of ClC-1. Our results reveal a mechanism of anion selectivity in ClC-Ka that is unique among CLC channels and antiporters. Given the overall similarity it is likely that these findings directly apply also to the ClC-Kb channel. Taken together these results represent an important progress for the understanding of the structure-function relationship of the kidney channels ClC-Ka and ClC-Kb and of CLC proteins in general.

Author contributions

G.Z. and A.P. designed the study, L.A., G.Z. and A.P. performed experiments and analyzed data, G.Z. and A.P. drafted and revised the manuscript; all authors approved the final version of the manuscript.

Acknowledgments

We thank Dr. Michael Pusch for helpful discussions and Dr. Raffaella Barbieri for assistance with molecular biology. The study was supported by the Telethon Carrier Award. A.P. is an Assistant Telethon Scientist at the Dulbecco Telethon Institute (TCP 14008, Telethon, Italy).

Disclosures

None.

References

1. Jentsch TJ, Pusch M. CLC Chloride Channels and Transporters: Structure, Function, Physiology, and Disease. *Physiological reviews* 2018; **98**(3): 1493-590.
2. Zifarelli G, Pusch M. CLC chloride channels and transporters: a biophysical and physiological perspective. *Rev Physiol Biochem Pharmacol* 2007; **158**: 23-76.
3. Uchida S, Sasaki S, Furukawa T, et al. Molecular cloning of a chloride channel that is regulated by dehydration and expressed predominantly in kidney medulla. *J Biol Chem* 1993; **268**(6): 3821-4.
4. Kieferle S, Fong P, Bens M, Vandewalle A, Jentsch TJ. Two highly homologous members of the CLC chloride channel family in both rat and human kidney. *Proc Natl Acad Sci U S A* 1994; **91**(15): 6943-7.
5. Estévez R, Boettger T, Stein V, et al. Barttin is a Cl⁻ channel beta-subunit crucial for renal Cl⁻ reabsorption and inner ear K⁺ secretion. *Nature* 2001; **414**(6863): 558-61.
6. Jentsch TJ. Chloride transport in the kidney: lessons from human disease and knockout mice. *J Am Soc Nephrol* 2005; **16**(6): 1549-61.
7. Rickheit G, Maier H, Strenzke N, et al. Endocochlear potential depends on Cl(-) channels: mechanism underlying deafness in Bartter syndrome IV. *EMBO J* 2008; **27**(21): 2907-17.
8. Waldegger S, Jeck N, Barth P, et al. Barttin increases surface expression and changes current properties of CLC-K channels. *Pflügers Arch* 2002; **444**(3): 411-8.
9. Scholl U, Hebeisen S, Janssen AG, Müller-Newen G, Alekov A, Fahlke C. Barttin modulates trafficking and function of CLC-K channels. *Proc Natl Acad Sci U S A* 2006; **103**(30): 11411-6.
10. Fischer M, Janssen AG, Fahlke C. Barttin activates CLC-K channel function by modulating gating. *J Am Soc Nephrol* 2010; **21**: 1281-9.
11. Gradogna A, Imbrici P, Zifarelli G, Liantonio A, Camerino DC, Pusch M. I-J loop involvement in the pharmacological profile of CLC-K channels expressed in *Xenopus* oocytes. *Biochimica et biophysica acta* 2014; **1838**(11): 2745-56.
12. Simon DB, Bindra RS, Mansfield TA, et al. Mutations in the chloride channel gene, CLCNKB, cause Bartter's syndrome type III. *Nat Genet* 1997; **17**(2): 171-8.
13. Birkenhäger R, Otto E, Schurmann MJ, et al. Mutation of BSND causes Bartter syndrome with sensorineural deafness and kidney failure. *Nat Genet* 2001; **29**(3): 310-4.
14. Schlingmann KP, Konrad M, Jeck N, et al. Salt wasting and deafness resulting from mutations in two chloride channels. *N Engl J Med* 2004; **350**(13): 1314-9.
15. Jeck N, Waldegger S, Lampert A, et al. Activating mutation of the renal epithelial chloride channel CLC-Kb predisposing to hypertension. *Hypertension* 2004; **43**(6): 1175-81.
16. Barlassina C, Dal Fiume C, Lanzani C, et al. Common genetic variants and haplotypes in renal CLCNKA gene are associated to salt-sensitive hypertension. *Hum Mol Genet* 2007; **16**(13): 1630-8.

17. Matsumura Y, Uchida S, Kondo Y, et al. Overt nephrogenic diabetes insipidus in mice lacking the CLC-K1 chloride channel. *Nat Genet* 1999; **21**(1): 95-8.
18. Grill A, Schiessl IM, Gess B, Fremter K, Hammer A, Castrop H. Salt-losing nephropathy in mice with a null mutation of the *Clcnk2* gene. *Acta Physiol (Oxf)* 2016; **218**(3): 198-211.
19. Hennings JC, Andrini O, Picard N, et al. The CLC-K2 Chloride Channel Is Critical for Salt Handling in the Distal Nephron. *J Am Soc Nephrol* 2017; **28**(1): 209-17.
20. Dutzler R, Campbell EB, Cadene M, Chait BT, MacKinnon R. X-ray structure of a CLC chloride channel at 3.0 Å reveals the molecular basis of anion selectivity. *Nature* 2002; **415**(6869): 287-94.
21. Dutzler R, Campbell EB, MacKinnon R. Gating the selectivity filter in CLC chloride channels. *Science* 2003; **300**(5616): 108-12.
22. Feng L, Campbell EB, Hsiung Y, MacKinnon R. Structure of a eukaryotic CLC transporters defines an intermediate state in the transport cycle. *Science* 2010; **330**(6004): 635-41.
23. Park E, Campbell EB, MacKinnon R. Structure of a CLC chloride ion channel by cryo-electron microscopy. *Nature* 2017; **541**(7638): 500-5.
24. Park E, MacKinnon R. Structure of the CLC-1 chloride channel from *Homo sapiens*. *eLife* 2018; **7**.
25. Picollo A, Pusch M. Chloride/proton antiporter activity of mammalian CLC proteins CLC-4 and CLC-5. *Nature* 2005; **436**(7049): 420-3.
26. Scheel O, Zdebik AA, Lourdel S, Jentsch TJ. Voltage-dependent electrogenic chloride/proton exchange by endosomal CLC proteins. *Nature* 2005; **436**(7049): 424-7.
27. Accardi A, Kolmakova-Partensky L, Williams C, Miller C. Ionic currents mediated by a prokaryotic homologue of CLC Cl⁻ channels. *J Gen Physiol* 2004; **123**(2): 109-19.
28. Zdebik AA, Zifarelli G, Bergsdorf EY, et al. Determinants of anion-proton coupling in mammalian endosomal CLC proteins. *J Biol Chem* 2008; **283**(7): 4219-27.
29. Zifarelli G, Pusch M. Conversion of the 2 Cl⁻/1 H⁺ antiporter CLC-5 in a NO₃⁻/H⁺ antiporter by a single point mutation. *EMBO J* 2009; **28**: 175-82.
30. Picollo A, Malvezzi M, Houtman JC, Accardi A. Basis of substrate binding and conservation of selectivity in the CLC family of channels and transporters. *Nat Struct Mol Biol* 2009; **16**(12): 1294-301.
31. De Angeli A, Monachello D, Ephritikhine G, et al. The nitrate/proton antiporter AtCLCa mediates nitrate accumulation in plant vacuoles. *Nature* 2006; **442**(7105): 939-42.
32. Bergsdorf E-Y, Zdebik AA, Jentsch TJ. Residues Important for Nitrate/Proton Coupling in Plant and Mammalian CLC Transporters. *J Biol Chem* 2009; **284**(17): 11184-93.
33. Wege S, Jossier M, Filleur S, et al. The proline 160 in the selectivity filter of the *Arabidopsis* NO₃⁻/H⁺ exchanger AtCLCa is essential for nitrate accumulation in planta. *Plant J* 2010; **63**(5): 861-9.
34. Ludewig U, Pusch M, Jentsch TJ. Two physically distinct pores in the dimeric CLC-0 chloride channel. *Nature* 1996; **383**(6598): 340-3.

- 1
2
3 35. Fahlke C, Desai RR, Gillani N, George AL, Jr. Residues lining the inner pore vestibule of
4 human muscle chloride channels. *J Biol Chem* 2001; **276**(3): 1759-65.
5
6 36. Lorenz C, Pusch M, Jentsch TJ. Heteromultimeric CLC chloride channels with novel
7 properties. *Proc Natl Acad Sci U S A* 1996; **93**(23): 13362-6.
8
9 37. Accardi A, Pusch M. Conformational changes in the pore of CLC-0. *J Gen Physiol* 2003;
10 **122**(3): 277-93.
11
12 38. Lin YW, Lin CW, Chen TY. Elimination of the slow gating of CLC-0 chloride channel by a
13 point mutation. *J Gen Physiol* 1999; **114**(1): 1-12.
14
15 39. Imbrici P, Liantonio A, Gradogna A, Pusch M, Camerino DC. Targeting kidney CLC-K
16 channels: pharmacological profile in a human cell line versus *Xenopus* oocytes. *Biochim Biophys*
17 *Acta* 2014; **1838**(10): 2484-91.
18
19 40. Gradogna A, Babini E, Picollo A, Pusch M. A regulatory calcium-binding site at the subunit
20 interface of CLC-K kidney chloride channels. *J Gen Physiol* 2010; **136**(3): 311-23.
21
22 41. Chen MF, Chen TY. Side-chain charge effects and conductance determinants in the pore of
23 CLC-0 chloride channels. *J Gen Physiol* 2003; **122**(2): 133-45.
24
25 42. Estévez R, Schroeder BC, Accardi A, Jentsch TJ, Pusch M. Conservation of chloride
26 channel structure revealed by an inhibitor binding site in CLC-1. *Neuron* 2003; **38**(1): 47-59.
27
28 43. Chen TY, Chen MF, Lin CW. Electrostatic control and chloride regulation of the fast gating
29 of CLC-0 chloride channels. *J Gen Physiol* 2003; **122**(5): 641-51.
30
31 44. Bennetts B, Parker MW. Molecular determinants of common gating of a CLC chloride
32 channel. *Nat Commun* 2013; **4**(2507): 1-11.
33
34
35
36
37
38
39
40
41
42
43
44
45
46
47
48
49
50
51
52
53
54
55
56
57
58
59
60

Figure legends

Figure 1. A) Top left panel. Dimeric structure of bClC-K (PDB entry: 5TQQ) viewed from the membrane plane (extracellular side above and cytoplasmic side below). The two subunits are shown in blu and green. Important residues and the ones analyzed in this work are represented as colored sticks in the blu subunit: S121 in green, V166 in red, Y425 in cyan, F519 in pink, Y520 in orange, N257 in dark red. The PDB entry for bClC-K did not include bound anions although an electron density was observed at S_{cen} but not S_{int} . The position of S_{cen} is conserved in bClC-K and EcClC-1²³. Here we superimposed the structure of bClC-K with the positions of the anions bound at S_{cen} and S_{int} as found in the structure of EcClC-1 (PDB entry: 1OTS) represented as magenta spheres with the purpose of illustrating the residues involved in anion coordination at S_{cen} in b-ClC-K. The other panels show an expanded representation of the anion permeation pathway of bClC-K, EcCLC-1 and CmCLC (PDB entry: 3ORG). In CmCLC, S_{cen} is occupied by the side chain of the “gating” glutamate, whereas anions are bound at S_{ext} and S_{int} . In all the panels some transmembrane helices were removed for clarity. B) Sequence alignment of the residues investigated in this work including their position in the secondary structure of bClC-K. They are S121, Y425, F519 and Y520 and are indicated in bold. The sequence alignment is based on the one of Feng et al.²² indicating a gap in α -helix R next to F519.

Figure 2. Representative patch-clamp recordings of wild-type ClC-Ka and the mutants S121G, S121T and S121P in extracellular solutions containing chloride (left) or nitrate (right).

Figure 3. A) Average of the ratio between the current amplitude in NO_3^- and the current amplitude in Cl^- measured at +80 mV for wild-type ClC-Ka and the mutants S121T, S121G and S121P. Values are 0.32 ± 0.02 (wild-type, n=10), 0.31 ± 0.05 (S121T, n=6), 0.29 ± 0.05 (S121G, n=6), 0.44 ± 0.02 (S121P, n=6). B) Average permeability ratio of NO_3^- relative to Cl^- obtained from the reversal potential of the currents under different ionic conditions according to Eq. 1 (see Methods).

Values are 0.32 ± 0.03 (wild-type), 0.28 ± 0.06 (S121T), 0.26 ± 0.03 (S121G) and 0.31 ± 0.06 (S121P). Number of experiments as in A).

Data were obtained for at list 3 batches of oocytes. Errors are indicated as SEM. Statistically significant differences compared to wild-type are indicated by an asterisk ($p < 0.01$).

Figure 4. Anion selectivity for wild-type CLC-Ka and the mutants Y520A, F519A and Y425A. The boxes display representative TEVC recordings in extracellular solution containing chloride (top left) or nitrate (bottom left) and I-V curves (right) for wild-type CLC-Ka (n=11), Y520A (n=7), F519A (n=10), Y425A (n=10). I-V curves were obtained from average steady-state currents in extracellular solutions containing chloride (black circles), nitrate (open circles), bromide (black triangles), iodide (black diamonds) with values normalized to those measured in chloride at + 80 mV. Data were obtained for at least 3 batches of oocytes ($n > 7$). Errors are indicated as SEM.

Figure 5. A) Average of the ratio between the current amplitude in NO_3^- and the current amplitude in Cl^- measured at +80 mV for wild-type CLC-Ka and the mutants N257A, Y520A, F519A, Y425A. Values are 0.65 ± 0.02 (wild-type, n=15), 0.11 ± 0.03 (N257A, n=15), 0.18 ± 0.03 (Y520A, n=7), 0.4 ± 0.03 (F519A, n=10), 1.3 ± 0.1 (Y425A, n=10). All values are significantly different from wild-type ($p < 0.01$). B) Average permeability ratio of NO_3^- relative to Cl^- obtained as in Figure 3. Values are 0.26 ± 0.02 (wild-type), 0.27 ± 0.03 (N257A), 0.36 ± 0.03 (Y520A), 0.41 ± 0.03 (F519A), 0.54 ± 0.05 (Y425A). Number of experiments as in A).

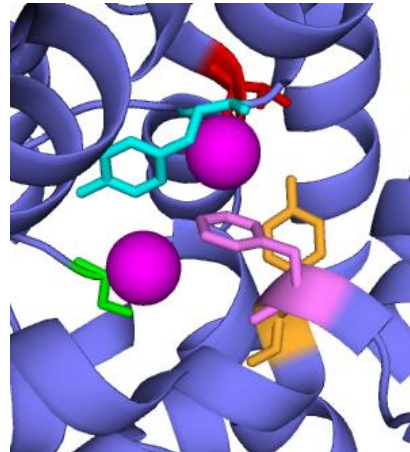
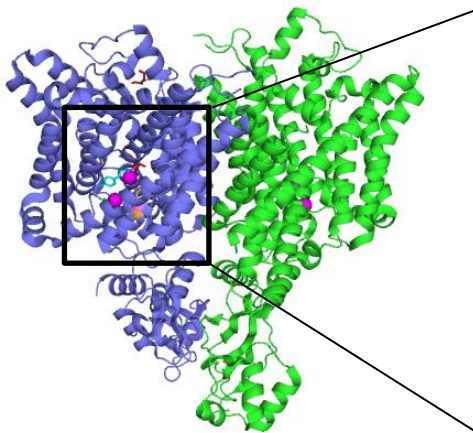
Data were obtained for at list 3 batches of oocytes. Errors are indicated as SEM. Statistically significant differences compared to wild-type are indicated by an asterisk ($p < 0.01$).

Figure 6. Nitrate selectivity for wild-type CLC-0 and the mutant A417Y. The boxes display representative TEVC recordings in extracellular solution containing chloride (top left) or nitrate (bottom left) and average I-V curves (right) for wild-type CLC-0 (n=11) and A417Y (n=7). I-V

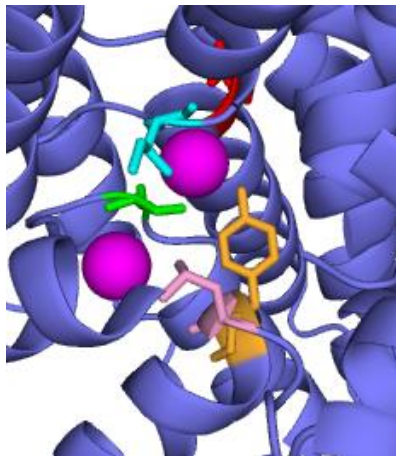
1
2
3 curves were obtained from average steady-state currents in extracellular solutions containing
4 chloride (black circles) and nitrate (open circles) with values normalized to those measured in
5 chloride at + 80 mV. Data were obtained for at least 3 batches of oocytes. Errors are indicated as
6
7
8
9 SEM.
10
11
12
13
14
15
16
17
18
19
20
21
22
23
24
25
26
27
28
29
30
31
32
33
34
35
36
37
38
39
40
41
42
43
44
45
46
47
48
49
50
51
52
53
54
55
56
57
58
59
60

A

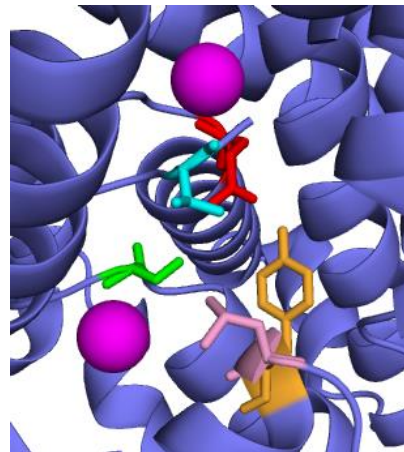
ClC-K



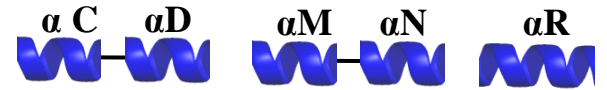
EcClC-1



CmClC



B



ClC-Ka	G S GIPE	AG Y FMP	S_ F YDG
ClC-Kb	G S GIPE	AG Y FMP	S_ F YDG
ClC-0	G S GIPE	CGAFVP	S_ L YDS
ClC-1	G S GIPE	CGGFMP	S_ L YDS
ClC-5	G S GIPE	SGLFIP	EG I YDA
ClC-7	G S GIPQ	AGVFIP	G_ L YDL
CmClC	G S GLPQ	AGVFVP	S_ L Y E T
EcClC-1	G S GIPE	GGIFAP	KPL Y SA

Figure 1

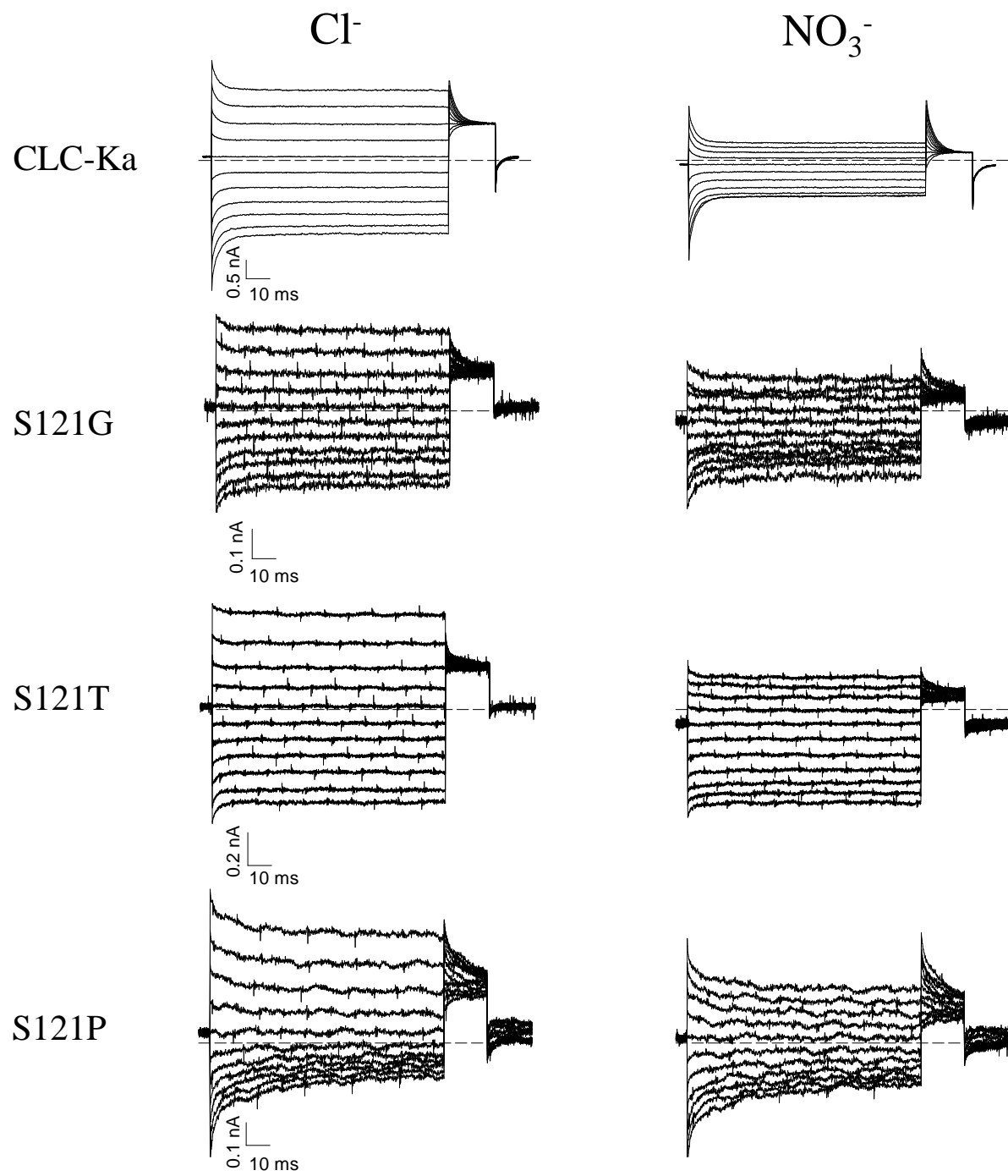
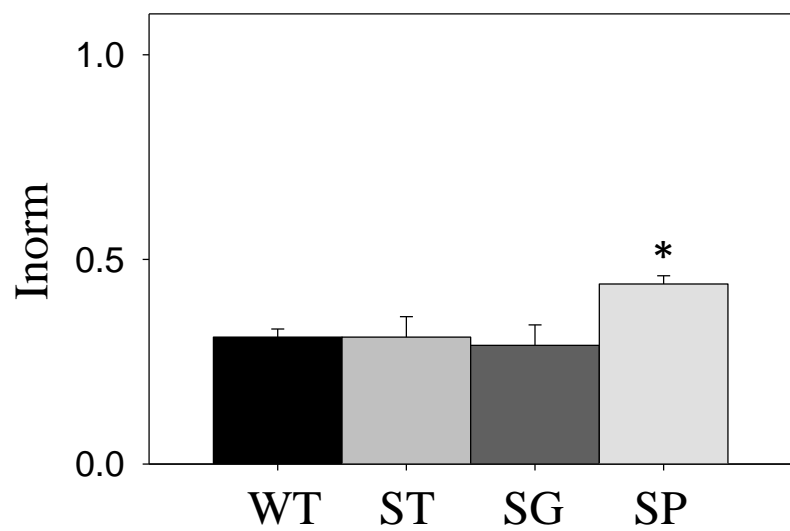


Figure 2

A



B

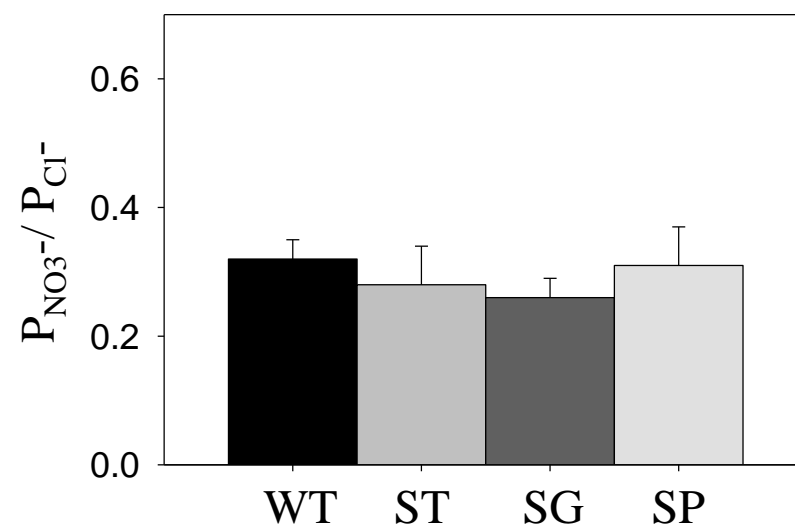


Figure 3

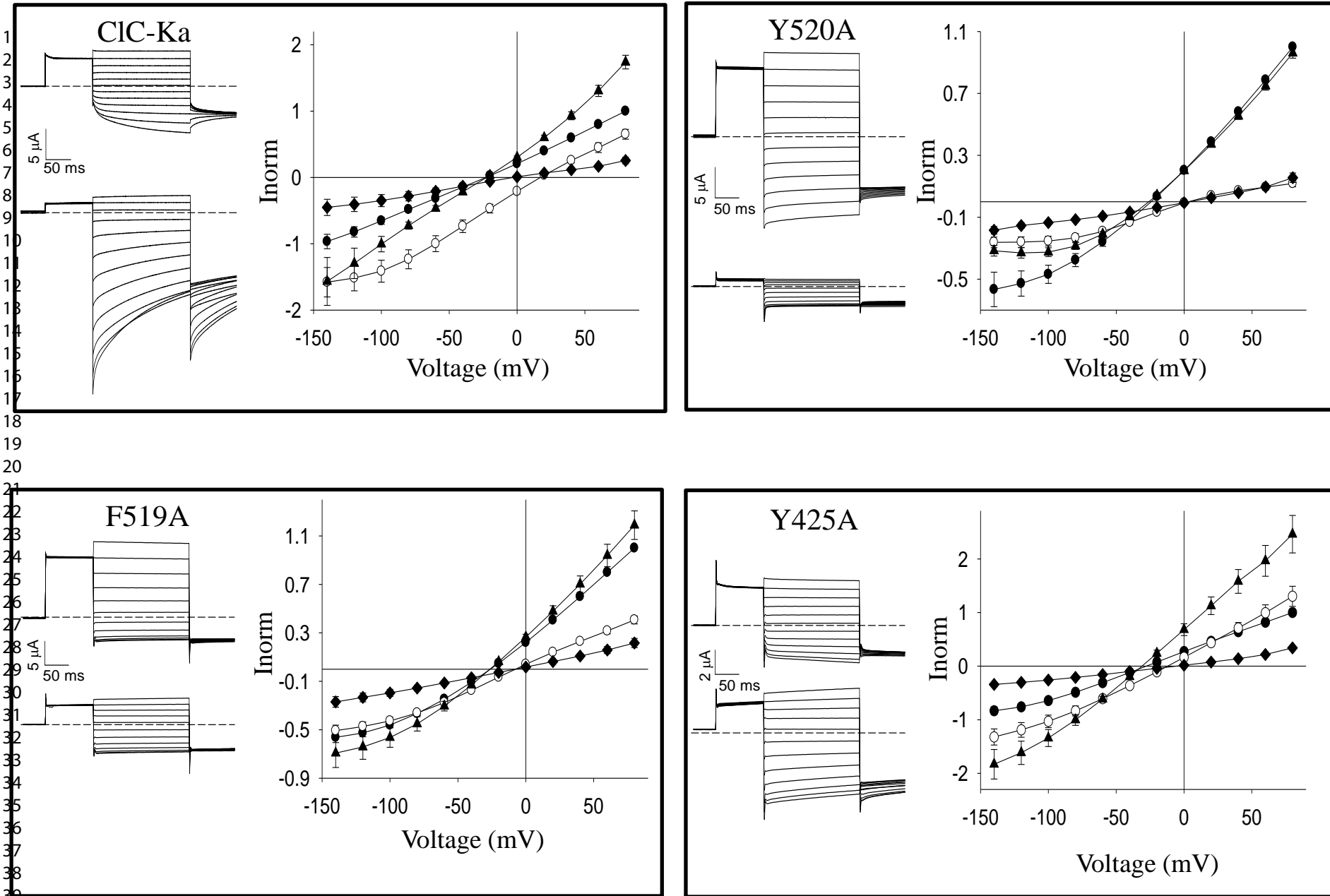
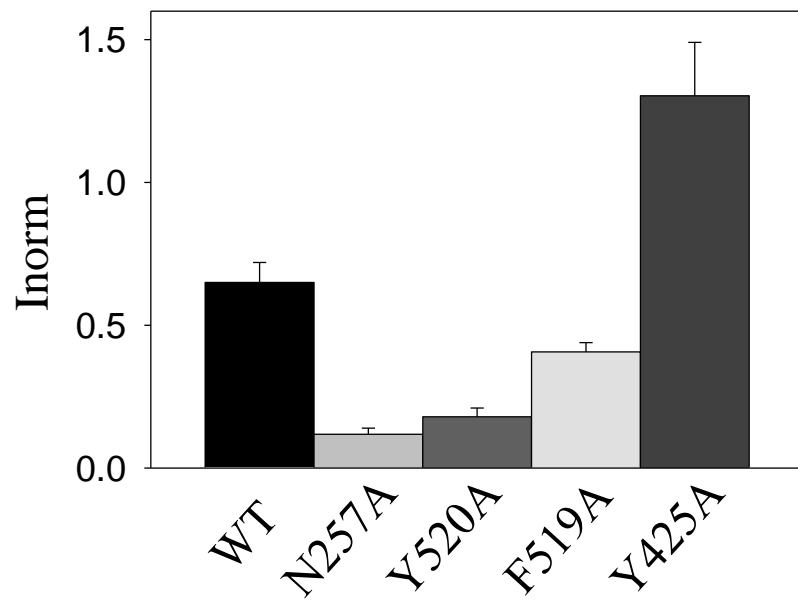


Figure 4

A



B

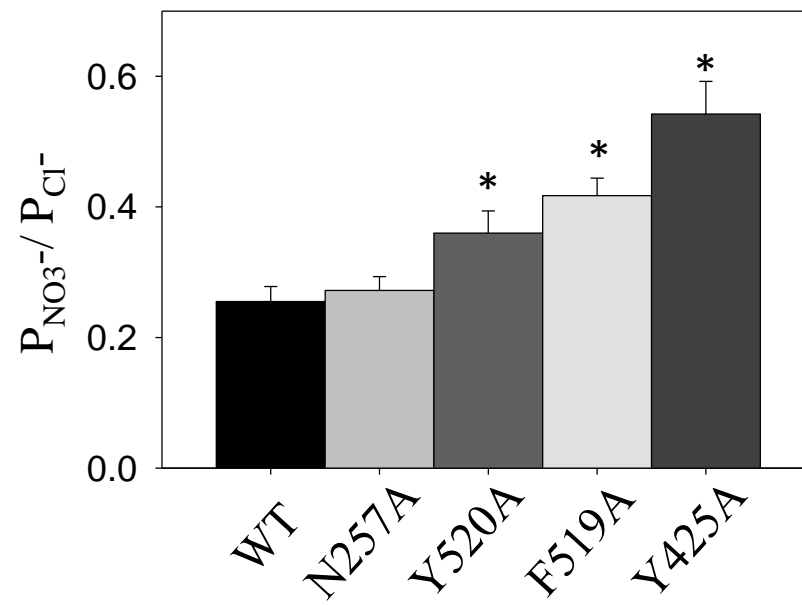


Figure 5

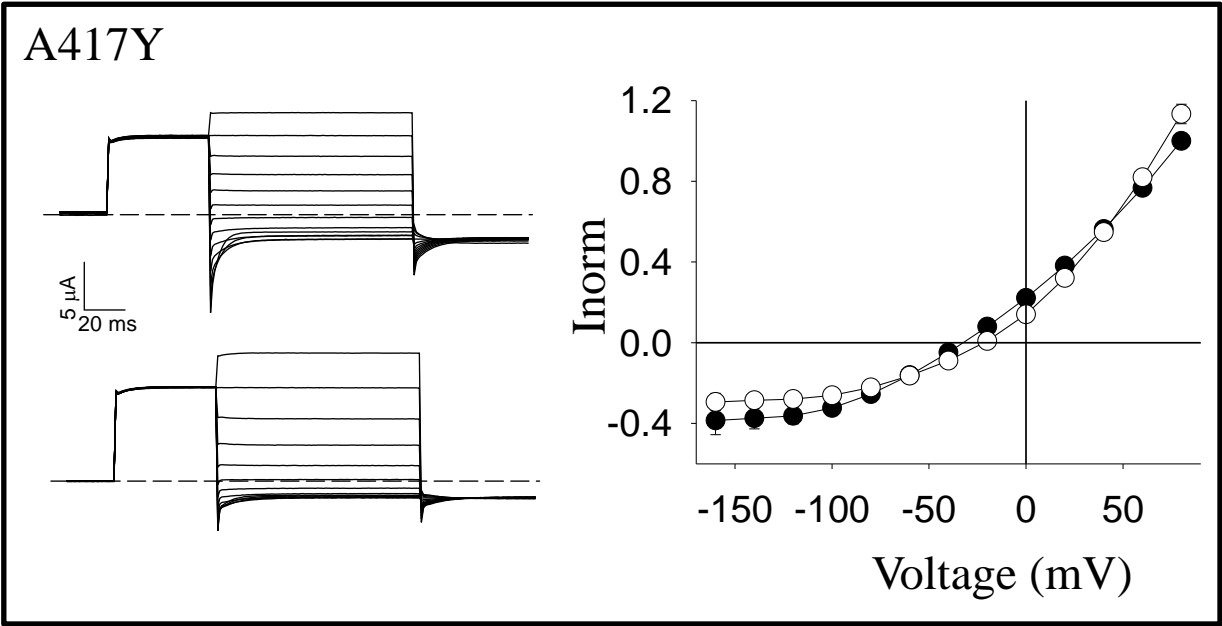
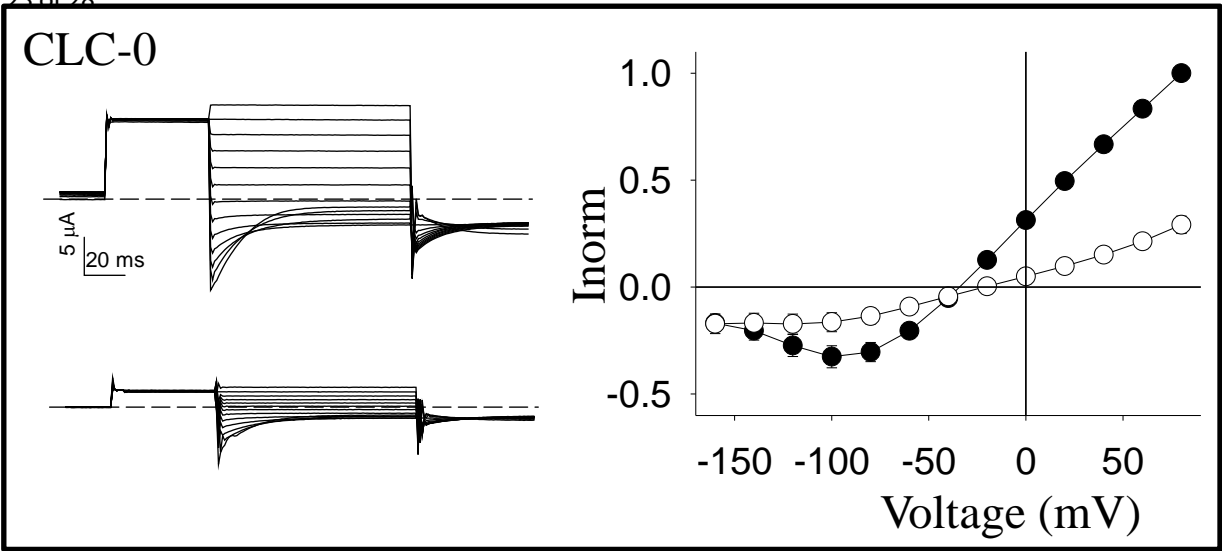
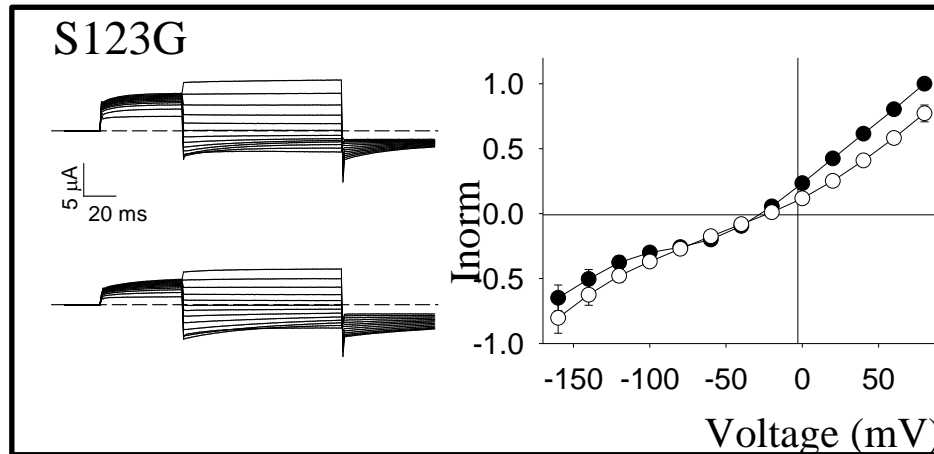
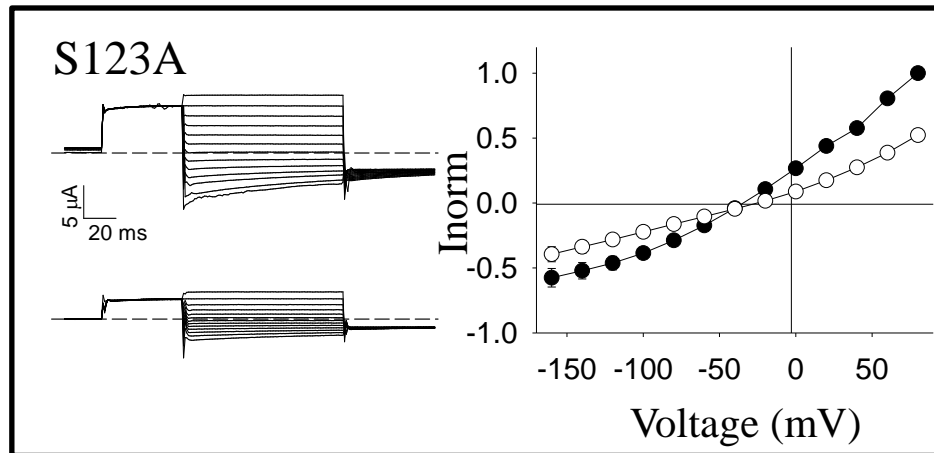
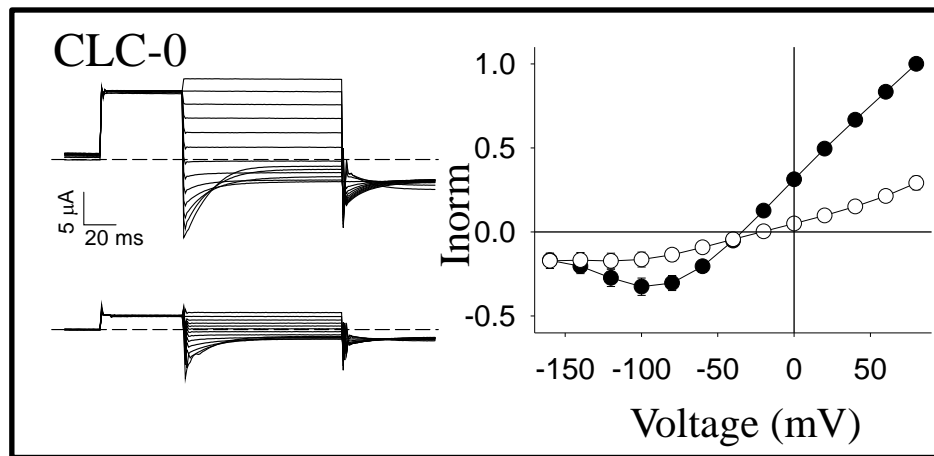
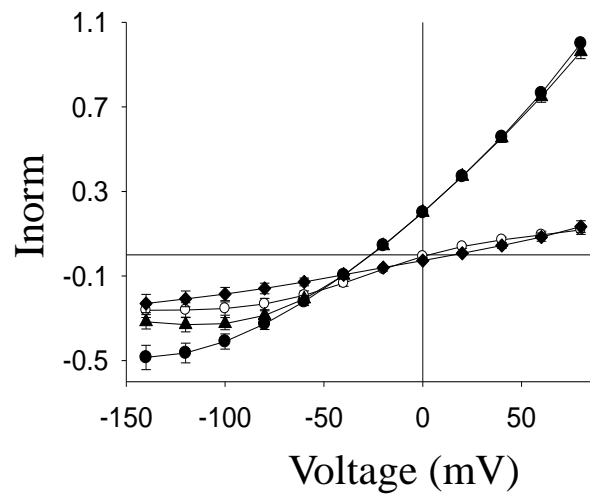
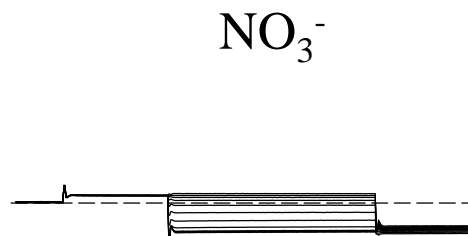
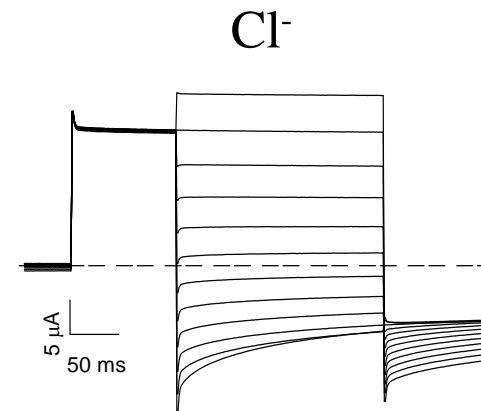


Figure 6



Suppl. Figure 1

ClC-Ka N257A

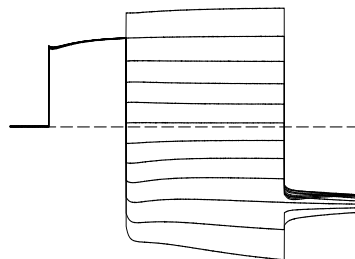
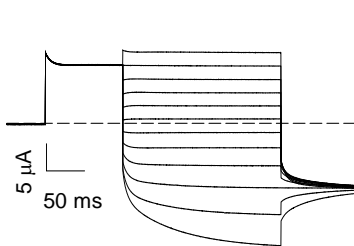


Suppl. Figure 2

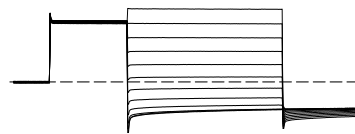
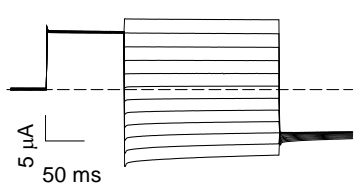
Cl⁻

Br⁻

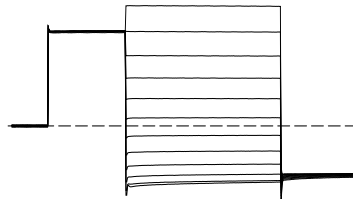
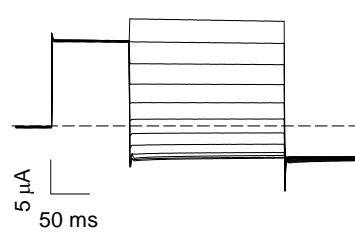
ClC-Ka



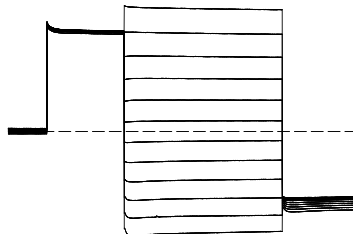
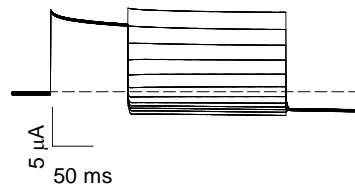
Y520A



F519A



Y425A



Suppl. Figure 3

Supplementary information

Supplementary table 1. Relative permeability of nitrate and bromide in respect to chloride for wild-type CLC-Ka and the mutants N257A, Y520A, F519A, Y425A.

	$P_{NO_3^-}/P_{Cl^-}$	P_{Br^-}/P_{Cl^-}
CLC-Ka (wild-type)	0.26 ± 0.02	1.1 ± 0.06
N257A	0.27 ± 0.02	1.01 ± 0.06
Y520A	0.36 ± 0.03	0.8 ± 0.05
F519A	0.41 ± 0.03	0.99 ± 0.01
Y425A	0.54 ± 0.05	1.06 ± 0.05

Supplementary Figure legends

Supplementary figure 1. Nitrate selectivity for wild-type CLC-0 and the mutants S123A and S123G. The boxes display representative TEVC recordings in extracellular solution containing chloride (top left) or nitrate (bottom left) and average I-V curves (right) for wild-type CLC-0 (n=8), S123A (n=10) and S123G (n=10). I-V curves were obtained from average steady-state currents in extracellular solutions containing chloride (black circles) and nitrate (open circles) with values normalized to those measured in chloride at + 80 mV. Values for $P_{NO_3^-}/P_{Cl^-}$ are 0.58 ± 0.02 , 0.72 ± 0.04 and 0.87 ± 0.01 for wild-type, S123A and S123G, respectively. Data were obtained for at least 3 batches of oocytes. Errors are indicated as SEM.

Supplementary figure 2. Anion selectivity for the CLC-Ka mutant N257A. The box displays representative TEVC recordings in extracellular solution containing chloride (top left), nitrate (top right left) or bromide (bottom left) and average I-V curves (bottom right). I-V curves were obtained from average steady-state currents in extracellular solutions containing chloride (black circles) (n=15), nitrate (open circles) (n=15), bromide (black triangles) (n=8), iodide (black diamonds) (n=8). Values were normalized to those measured in chloride at + 80 mV. Data were obtained for at least 3 batches of oocytes. Errors are indicated as SEM.

Supplementary figure 3. Representative TEVC recordings for wild-type ClC-Ka and the mutants Y520A, F519A and Y425A in extracellular solution containing chloride (left) and bromide (right). The changes in current levels in bromide were fully reversible.